CHR11, a chromatin-remodeling factor essential for nuclear proliferation during female gametogenesis in *Arabidopsis thaliana*

Wilson Huanca-Mamani*, Marcelina Garcia-Aguilar*, Gloria León-Martínez*, Ueli Grossniklaus†‡, and Jean-Philippe Vielle-Calzada*§¶

*Laboratory of Reproductive Development and Apomixis, Department of Genetic Engineering, Centro de Investigación y de Estudios Avanzados–Unidad Irapuato, Apartado Postal 629, CP 36500, Irapuato, Guanajuato, Mexico; †Cold Spring Harbor Laboratory, 1 Bungtown Road, Cold Spring Harbor, NY 11724; and ‡Institute of Plant Biology and Zurich–Basel Plant Science Center, University of Zurich, Zollikerstrasse 107, CH-8008 Zurich, Switzerland

Communicated by Luis Herrera-Estrella, National Polytechnic Institute, Guanajuato, Mexico, September 19, 2005 (received for review May 9, 2005)

Chromatin-remodeling factors regulate the establishment of transcriptional programs during plant development. Although 42 genes encoding members of the SWI2/SNF2 family have been identified in *Arabidopsis thaliana*, <10 have been assigned a precise function on the basis of a mutant phenotype, and none have been shown to play a specific role during the gametophytic phase of the plant life cycle. *A. thaliana* chromatin-remodeling protein 11 (*CHR11*) encodes an imitation of switch (ISWI)-like chromatin-remodeling protein abundantly expressed during female gametogenesis and embryogenesis in *Arabidopsis*. To determine the function of *CHR11* in wild-type plants, we introduced a hairpin construct leading to the production of double-stranded RNA, which specifically degraded the endogenous *CHR11* mRNA by RNA interference (RNAi). Transcription of the RNAi-inducing hairpin RNA was driven by either a constitutive cauliflower mosaic virus 35S promoter (CaMV35S) acting at most stages of the sporophytic phase or a newly identified specific promoter acting at the onset of the female gametophytic phase (pFM1). All adult transformants that constitutively lacked sporophytic *CHR11* activity showed reduced plant height and small cotyledonary embryos with limited cell expansion. In contrast, RNAi lines in which *CHR11* was specifically silenced at the onset of female gametogenesis (megagametogenesis) had normal height and embryo size but had defective female gametophytes arrested before the completion of the mitotic haploid nuclear divisions. These results show that *CHR11* is essential for haploid nuclear proliferation during megagametogenesis and cell expansion during the sporophytic phase, demonstrating the functional versatility of SWI2/SNF2 chromatin-remodeling factors during both generations of the plant life cycle.

imitation of switch proteins | megagametophyte | RNA interference | seed development | functional megaspore

The accessibility of DNA to transcription factors or other types of interacting molecules is regulated by enzymatic complexes that modify nucleosomal structure by means of ATP-dependent chromatin-remodeling or histone modification (1). ATP-dependent chromatin-remodeling factors are multisubunit complexes that alter the chromatin structure by changing the conformational state of the nucleosome. These structural changes are accomplished without covalent modification and can be involved in either the activation or the repression of transcription (2). Members of the SWI2/SNF2 family of ATP-dependent proteins share an ATPase domain that is essential for their chromatin-remodeling activity. In addition, SWI2/SNF2 proteins have a large variety of N- and C-terminal domains that are often involved in their interaction with other members of specific chromatin-associated complexes. The largest eukaryotic group of SWI2/SNF2, ATP-dependent, chromatin-remodeling proteins is the imitation of switch (ISWI) subfamily. Originally identified in *Drosophila* (3, 4), ISWI members are distinguished from other SWI2/SNF2 proteins by the presence of the SANT domain in their C-terminal region. The SANT domain was originally identified in several metazoan proteins that include SWI3, ADA2, N-CoR TFIIIB″, and ISWI (5). From yeast to humans, different portions of the SANT domain are required for interaction either with histone deacetylases/acetyltransferases (the N-terminal portion) or directly with chromatin (the C-terminal portion) (6–8). ISWI proteins have been shown to accomplish many different functions, including transcriptional activation and repression, the assembly of chromatin structure, the replication of heterochromatin, and the cohesion of sister chromatids (9).

Chromatin-remodeling factors have been shown to regulate the establishment of transcriptional programs at many developmental stages of the plant life cycle. Although 42 genes encoding SWI2/SNF2 proteins have been identified in the genome of *Arabidopsis thaliana* [including members of all conserved subfamilies SNF2, DDM1, ISWI, CHD, and SRCAP (www.chromdb.org)] (10), <10 have been assigned a precise function on the basis of a mutant phenotype (11), and none have been shown to play a direct and specific role during the gametophytic phase of the life cycle. Several SWI2/SNF2 proteins are known to be involved in the regulation of epigenetic mechanisms of plant development. For example, mutations in *DECREASED IN DNA METHYLATION 1* (*DDM1*) cause a 70% reduction of genomic cytosine methylation and lead to morphological abnormalities in the course of inbreeding because of the accumulation of genetic and epigenetic alterations (12–15). Similarly, *DRD1* encodes a chromatin-remodeling factor involved in RNA-guided DNA cytosine methylation (16). In contrast, *MORPHEUS MOLECULE 1* (*MOM1*) is required for the maintenance of transcriptional gene silencing but does not affect regular methylation patterns (17). *GYMNOS/PICKLE* encodes an SWI2/SNF2-like protein of the CHD subfamily that acts as a repressor of meristematic genes and embryonic fate (18, 19). Three additional SWI2/SNF2 family members have been implicated in the temporal regulation of key developmental transitions during the plant life cycle. *SPLAYED* (*SYD*) controls the transition between vegetative and reproductive development and is required for normal carpel and ovule formation (20). *syd* mutants show a wide range of pleiotropic effects, indicating that specific SWI2/SNF2 members regulate a wide range of transcriptional events. Recently, *SYD* was shown to control cell fate in the shoot apical meristem by directly regulating the transcription of the master regulator *WUSCHEL* (21). *AtBRAHMA* controls plant size and flowering time through repression of a photoperiod-dependent flowering pathway (22). Finally, *PHOTOPERIOD-INDEPENDENT EARLY FLOWER-*

Conflict of interest statement: No conflicts declared.

Abbreviations: CHR11, *Arabidopsis* chromatin-remodeling protein 11; CHR17, *Arabidopsis* chromatin-remodeling protein 17; ISWI protein, imitation of switch protein; RNAi, RNA interference; GUS, β-glucuronidase; siRNA, short interfering RNA fragment.

§Present address: National Laboratory for Genomic Biodiversity, Langebio, Apartado Postal 629, 36500 Irapuato, Mexico.

¶To whom correspondence should be addressed. E-mail: vielle@ira.cinvestav.mx.

PLANT BIOLOGY

ING 1 (*PIE1*) is the only ISWI family gene that has been functionally characterized in flowering plants. *pie1* loss-of-function mutants show premature flowering in noninductive photoperiods independently of *FLOWERING LOCUS C* (*FLC*), a floral repressor acting at the intersection of multiple floral regulatory pathways (23).

In this article, we report that *CHR11*, a constitutively expressed gene that encodes a member of the ISWI class of chromatin-remodeling proteins, participates in developmental processes during the diploid (sporophytic) and the haploid (gametophytic) phase of the *Arabidopsis* life cycle. To determine the function of *CHR11*, we introduced a hairpin construct in wild-type plants that leads to the production of double-stranded RNA, which specifically degraded the endogenous *CHR11* mRNA by RNA interference (RNAi). Transcription of the RNAi-inducing hairpin RNA was driven either by a constitutive promoter acting at most stages of the sporophytic phase or by a specific promoter acting at the onset of the female gametophytic phase. All adult transformants that constitutively lacked sporophytic *CHR11* activity showed reduced plant height and small cotyledonary embryos with limited cell expansion. In contrast, RNAi lines in which *CHR11* was specifically silenced at the onset of megagametogenesis had normal height and embryo size but had defective megagametophytes arrested before completion of the mitotic haploid nuclear divisions. Our results assign sporophytic and gametophytic functions to a gene encoding a member of the ISWI family of chromatin-remodeling factors.

Materials and Methods

Plant Material. Plants were grown on a 3:1:1 mixture of Mix3-Sunshine (SunGro, Bellevue, WA), vermiculite, and perlite (vol/vol/vol ratio) containing 1.84 kg/m^3 of 14-14-14 slow-release fertilizer (Osmocote, Sierra, Marysville, OH) under greenhouse conditions or in a Percival incubator (Percival Scientific, Perry, IA) at 19°C with a photoperiod of 16 h of light and 8 h of dark. Primary transformant seedlings were selected by using 0.05% of BASTA herbicide. Subsequent transformant generations were selected in Murashige and Skoog (MS) medium containing 10 μg/ml glufosinate ammonium (Crescent chemical, Islandia, NY) in a Percival incubator under the same photoperiod conditions.

RNA Isolation and Analysis. Total RNA was isolated by grinding tissue in liquid nitrogen in the presence of TRIzol (Invitrogen). For RT-PCR analysis, 5 μg of total RNA from developing siliques was used to synthesize first-strand cDNA by using an oligo(dT) primer (Sigma). The following primers were used for specific cDNA amplification: *CHR11* (At3g06400), CHR11-sense5 (5′-TTACGGATCTGTCGAGTC-3′) and CHR11-antisense5 (5′-TTACGGAAGAGAAGTCTAC-3′); *CHR17* (At5g18620), CHR17-sense2 (5′-AGGCTTGTGTTGAATCCAT-3′) and CHR17-antisense2 (5′-GAGAAGTCGGAGACAATG-3′); and *ACT11* (At3g12110), ACT11-sense (5′-TTCAACACTCCTGCCATG-3′) and ACT11-antisense (5′-TGCAAGGTCCAAACGCAG-3′). Agarose gels stained with ethidium bromide were blotted onto Hybond N$^+$ membranes and hybridized at 65°C with a [^{32}P]cDNA probe specific to each gene tested. After exposure (3 days), autoradiograms were digitally scanned, and the intensity of the signals was assessed by using LABSWORKS 3.0.02 (Microsoft). For Northern blot analysis, 20 μg of total RNA was isolated and processed as described in ref. 24. For detection and analysis of small RNA fragments, total RNA from developing flowers was enriched for low-molecular-weight RNAs by using Hamilton's solution, as described in refs. 25 and 26. A total of 60 μg of low-molecular-weight RNA was separated in 15% polyacrylamide·8 M urea gels, electroblotted onto a ZETA-PROBE membrane (Bio-Rad) overnight at 24 V and 4°C, and crosslinked by using UV irradiation. The membranes were hybridized at 65°C to a 570-bp randomly primed, ^{32}P-labeled cDNA fragment corresponding to the *CHR11* coding region.

Generation of RNAi Plasmids. A 542-bp cDNA fragment corresponding to nucleotides 1244–1786 of the *CHR11* coding region was amplified by RT-PCR and cloned in TOPO-PCRII (Invitrogen). For cDNA amplification, we used following the primers: CHR11-sense4 (5-CGAA**CCATGGTCTAGA**CGAAGAAGGAGACCATAC; containing restriction sites NcoI and XbaI in boldface) and CHR11-antisense4 (TT**GGCGCGCCGGATCC**TTGCAAGTCGACTTGTGG; containing restriction sites AscI and BamHI in boldface). After digesting with NcoI and AscI, the amplified *CHR11* fragment was cloned in pFGC5941 in sense orientation (27). To identify the insertion site in enhancer detector line ET499, thermal asymmetric interlaced PCR (28) was performed as described in ref. 29. To isolate the pFM1 promoter, primers pET499-S1 (5′-TA**AAGCTT**CATACTAGCATGTATCCAC; containing the restriction site HindIII in boldface) and pET499-AS1 (5′-TA**GGATCC**GGTGGAACTTTATCGGTTT; containing the restriction site BamHI in boldface) were used to amplify an 880-bp genomic fragment in the 5′ region of At4g12250. The fragment was subsequently cloned in TOPO-PCRII and pBI101.2 (30). To generate the *pFM1*::*CHR11*-RNAi cassette, primers p499-S3 (5′-GC**GAATTC**ATACTAGCATGTATCCAC; containing the restriction site EcoRI in boldface) and p499-AS2 (5′-CATG**CCATGG**TGGAACTTTATCGGTTT; containing the restriction site NcoI in boldface) were used to amplify pFM1 from genomic DNA. The pFGC5941 plasmid (27) was digested with EcoRI and NcoI to excise the CaMV35S promoter, and the pFM1 promoter was inserted into the same plasmid by using the EcoRI and NcoI restriction sites.

***In Situ* Hybridization.** A specific 156-bp fragment corresponding to a portion of the *CHR11* 3′ UTR was amplified by PCR using primers CHR11-sense5 (5′-TTACGGATCTGTCGAGTC) and CHR11-antisense5 (5′-TTACGGAAGAGAAGTCTAC) and subsequently cloned in TOPO-PCRII. The resulting plasmid was linearized with SstI (antisense) and BamHI (sense) and used for generating digoxigenin-labeled probes. *In situ* hybridization was performed as described in ref. 31.

Histological Analysis. For semithin sections, mature seeds were fixed in 3% glutaraldehyde for 2 h, rinsed in 50 mM cacodylate buffer, and postfixed in 2% osmium tetroxide (in the same buffer). After dehydration in an acetone series, specimens were embedded in Spurr's resin, sectioned at thicknesses of 1 and 2 μm on a Leica-Ultracut-R ultramicrotome (Deerfield, IL), and observed on a Leica-DMR microscope under a bright field. For whole-mount observations, individual gynoecia were dissected longitudinally by using hypodermic needles (1-ml insulin syringes, Becton Dickinson) and processed as described in ref. 32. β-Glucuronidase (GUS) staining assays were conducted as described in ref. 33. The surface area and total length of a group of at least 20 wild-type or *CHR11*-RNAi embryos were measured by using the image processing and analysis feature in JAVA (IMAGE-J), as described in ref. 34.

Results and Discussion

***CHR11* Is Abundantly Expressed During the Sporophytic and Gametophytic Phases.** On the basis of the presence of the SANT domain, three genes belonging to the ISWI family have been identified in *Arabidopsis*: *CHR11* (At3g06400), *CHR17* (At5g18620), and *PIE1* (At3g12810; www.chromdb.org). Fig. 1 illustrates the predicted domain structures of the proteins encoded by these three genes and indicates their degree of amino acid similarity, taking CHR11 as a reference. Like CHR17 and PIE, CHR11 has the SNF2 and HEL-C domains that together constitute the SWI/SNF ATPase domain present in all SWI2/SNF2 chromatin-remodeling proteins. The C-terminal portion of all three proteins harbors the SANT domain characteristic of ISWI-like proteins. Although CHR11 and CHR17 show a high degree of

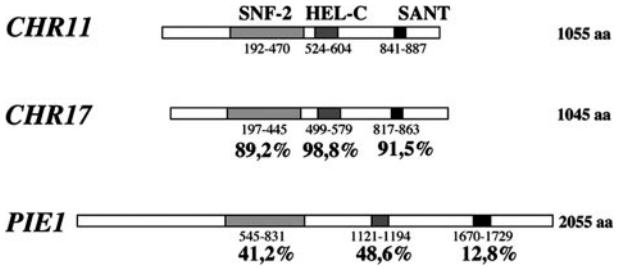

Fig. 1. Organization and comparison of ISWI-like proteins in *Arabidopsis*. Locations of conserved domains with significant homologies are indicated by boxes: SNF2 (light gray), HEL-C (dark gray), and SANT (black). The percentages indicate the degree of amino acid similarity for each conserved domain, taking CHR11 as a reference. Numbers below each protein indicate the initial and final codon of the corresponding domains.

amino acid similarity in all three domains, PIE1 has limited similarity with both proteins. Publicly available expression profiles generated by microarray analysis indicate that *CHR11* and *CHR17* are constitutively expressed (www.genevestigator.ethz.ch/); however, *CHR11* is invariably expressed at significantly higher levels than *CHR17*, being 2× more abundant in rosette leaves and up to 4× more abundant in mature flowers and stems (35). We confirmed the constitutive expression of both genes by RT-PCR analysis (data not shown).

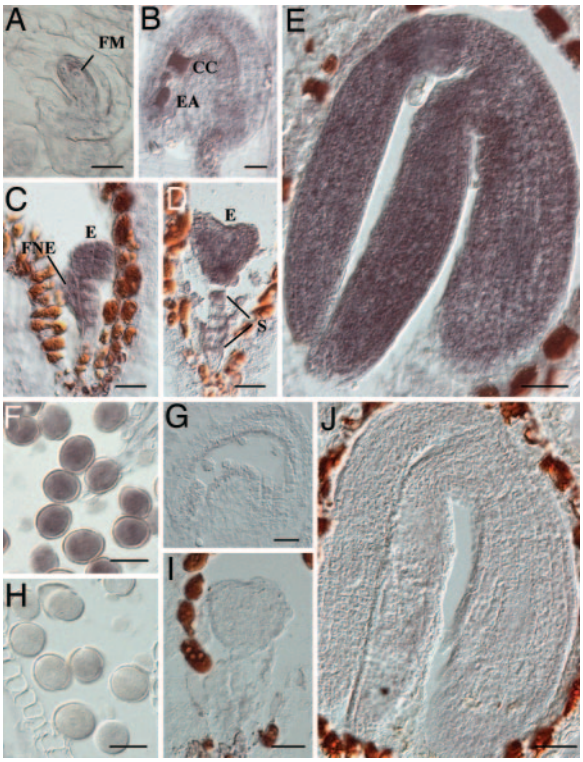

Fig. 2. Localization of *CHR11* mRNA by *in situ* hybridization. (*A–F*) Hybridizations with antisense probe. (*A*) Developing ovule at the end of megasporogenesis. (*B*) Mature ovule with a fully differentiated megagametophyte. (*C*) Seed at the globular embryo stage. (*D*) Seed at the early heart embryo stage. (*E*) Mature seed with a fully differentiated cotyledonary embryo. (*F*) Mature pollen. (*G–J*) Hybridizations with sense probe. (*G*) Mature ovule with a fully differentiated megagametophyte. (*H*) Mature pollen. (*I*) Seed at the transition embryo stage. (*J*) Mature seed with a fully differentiated cotyledonary embryo. CC, central cell; E, embryo; EA, egg apparatus; FM, functional megaspore; FNE, free nuclear endosperm; S, suspensor. (Scale bars: *A–D* and *F–I*, 20 μm; *E* and *J*, 40 μm.)

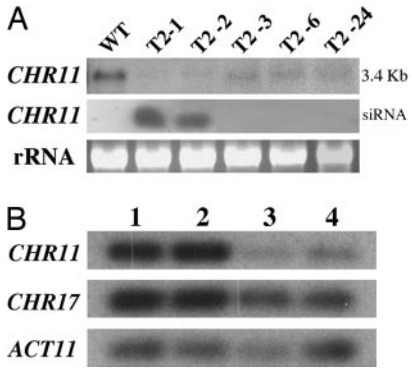

Fig. 3. Accumulation of CHR11 transcripts, the presence of 21-bp small RNAs, and specific *CHR11* silencing in constitutive *CHR11*-RNAi T2 lines. (*A*) Expression analysis of five *CHR11*-RNAi T2 lines and a wild-type control (WT). *CHR11* mRNA abundance is shown (*Upper*) and the detection of siRNAs corresponding to *CHR11* is shown (*Middle*). Control rRNA in ethidium bromide gel is also shown (*Bottom*). (*B*) Posttranscriptional gene silencing is specific to *CHR11*. RNA extracted from wild-type siliques (lanes 1 and 2) or T3-2 *CHR11*-RNAi siliques (lanes 3 and 4) and containing globular to heart stage embryos (lanes 1 and 3) or mature cotyledonary embryos (lanes 2 and 4). After cDNA synthesis, PCR amplification was performed with primers specific to *CHR11*, *CHR17*, or *ACT11*. Agarose gels were blotted and probed with a corresponding gene. *ACT11* was used as positive control.

To determine the spatial and temporal pattern of expression of *CHR11*, we characterized the mRNA localization patterns of *CHR11* by *in situ* hybridization. To avoid the localization of *CHR17* mRNA, digoxigenin-labeled probes were generated by using a distinctive portion of the *CHR11* 3′ UTR. In the developing ovule, *CHR11* was initially expressed in all cells of the young nucellus, including the functional megaspore (Fig. 2*A*). After the initiation of megagametogenesis, *CHR11* mRNA was localized in most cells of the ovule, including the integuments, the developing megagametophyte, and the funiculus. In mature ovules, *CHR11* expression was particularly strong in the cellularized megagametophyte (Fig. 2*B*). After double fertilization, *CHR11* expression persisted in the developing embryo and the free nuclear endosperm until seed maturity (Fig. 2 *C–E*). *CHR11* mRNA was also abundantly expressed in developing male gametophytes and mature pollen grains (Fig. 2*F*) but not in the tapetum or other sporophytic tissues of the fully differentiated anther. These results indicate that *CHR11* is abundantly expressed in both sporophytic and gametophytic tissues throughout reproductive development.

Generation of Constitutive *CHR11*-RNAi Lines and Analysis of RNA Levels. To determine a possible sporophytic function of *CHR11* in *Arabidopsis*, a 542-bp fragment of the *CHR11* cDNA was cloned into a pFGC5941 RNAi vector in both sense and antisense orientation and used to transform wild-type Columbia plants (27, 32). In pFGC5941, transcription of a partial *CHR11* sequence is driven by a 35S promoter of the cauliflower mosaic virus (CaMV35S) and results in posttranscriptional gene silencing. A total of 42 adult primary transformants were generated, all of which showed reduced height when compared with the wild type, a defect that was consistently maintained in the T2 and T3 generations. To determine a possible relationship between a decrease in *CHR11* transcript levels and the observed defective phenotype, RNA was extracted from developing floral buds and flowers of BASTA-resistant *CHR11*-RNAi T2 lines and used for RNA gel blot analysis. Compared with wild-type plants, all five T2 lines analyzed showed substantial decrease in the transcript levels of *CHR11* (Fig. 3*A*). Polyacrylamide gels were used to detect the presence of short interfering RNA fragments (siRNAs) corresponding to *CHR11*. siRNAs corresponding to *CHR11* were detected in T2-1 and T2-2,

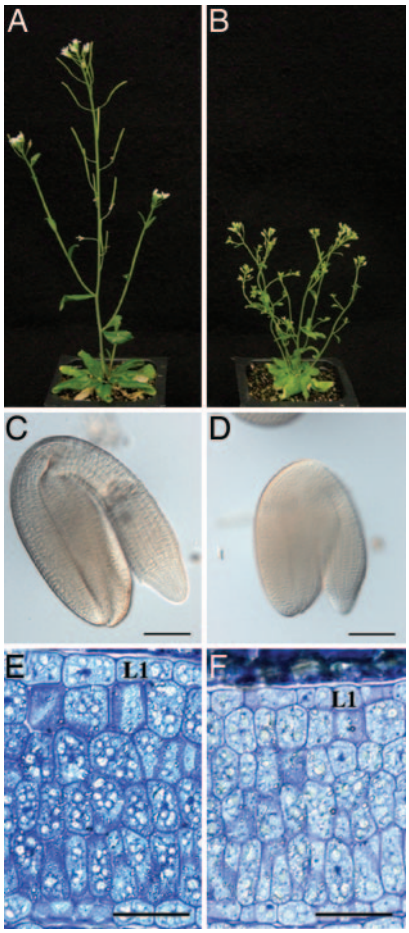

Fig. 4. Plant height and cell size are reduced in constitutive *CHR11*-RNAi lines. (*A*) An adult wild-type plant. (*B*) An adult plant of *CHR11*-RNAi T2-2 showing reduced height. (*C*) A mature cotyledonary wild-type embryo. (*D*) A mature cotyledonary embryo of *CHR11*-RNAi T4-2 showing reduced length and surface area. (*E*) A semithin transversal section of a wild-type cotyledon in a mature embryo. (*F*) A semithin transversal section of an embryo in *CHR11*-RNAi T4-2 showing reduced cell expansion. (Scale bars: *C* and *D*, 500 μm; *E* and *F*, 100 μm; *G* and *H*, 30 μm.)

two lines showing strong defects in height but not in wild-type plants or other *CHR11*-RNAi T2 lines, confirming that the absence of mRNA expression can be associated with the degradation of the corresponding transcript (Fig. 3*A*). The absence of siRNA detection in plants showing defective phenotypes could be explained by a fast siRNA turnover in lines with multiple T-DNA insertions (27). Because the homology between *CHR11* and *CHR17* is 89% at the nucleic acid level in the region targeted, we performed RT-PCR in the wild-type line and in the selected line *CHR11*-RNAi T3-2 lines showing small embryos. To assess the levels of gene expression, we blotted the RT-PCR and hybridized the resulting membranes with radiolabeled *CHR11*- or *CHR17*-specific probes. Although a slight decrease of $<15\%$ in signal intensity was detected in embryos of *CHR11*-RNAi lines (Fig. 3*B*), *CHR11* expression was reduced to $<10\%$ at both developmental stages tested, demonstrating that in *CHR11*-RNAi lines, posttranscriptional gene silencing mainly affects *CHR11*.

Plant Height and Cell Size Are Reduced in Constitutive *CHR11*-RNAi Lines. Primary *CHR11*-RNAi transformants were partially stunted and their maximum height was significantly lower than in the wild type. Although wild-type individuals reached a maximum mean height of 54.18 cm ($\pm$5 cm, $n = 11$), *CaMV35S*::*CHR11*-RNAi lines had a maximum mean height of 39.2 cm ($\pm$7.5 cm, $n = 8$; Fig. 4 *A* and *B*). To determine whether the defect originated early during development, whole-mounted mature embryos from the wild type and the T4 generation of the previously selected lines (*CHR11*-RNAi T4-1 and T4-2) were analyzed to compare their size on the basis of the estimation of their area and their linear length, including the radicle and the cotyledons. Although wild-type embryos have a mean length of 992.4 μm ($\pm$42.5 μm, $n = 20$) and a mean maximum surface area of 7,950 μm^2 ($\pm$578 μm^2, $n = 20$), *CHR11*-RNAi lines had lengths between 837 and 883.2 μm ($\pm$52.3 and $\pm$53.2 μm for T4-1 and T4-2, respectively, $n = 20$) and maximum surface areas ranging between 6,013 and 6,714 μm^2 ($\pm$667 and $\pm$514 μm^2 for T4-1 and T4-2, respectively, $n = 20$; Fig. 4 *C* and *D*). To determine the cytological nature associated with these size differences, we analyzed semithin sections of fixed mature cotyledons in ungerminated embryos. No differences in the overall pattern of cell division between wild type and *CHR11*-RNAi embryos were identified. The same number of cell layers and an indistinguishable number of cells per layer were found in mature cotyledons of both samples; however, cells of defective embryos were smaller than those of the wild type not only in the cotyledons but also in the radicle and the meristem. These differences were particularly evident in the L1 layer of the cotyledons (Fig. 4 *E* and *F*). Although wild-type L1 cells had a mean surface area of 2,447 $\pm$ 182 μm^2, L1 cells in mature embryos of line T4-2 had a mean surface area of 579 $\pm$ 202 μm^2. All differences in plant height, embryo length, embryo surface area, and L1 cell surface area were confirmed to be statistically significant by using χ^2 analysis. Overall, these results indicate that the activity of *CHR11* is necessary for normal cell expansion during late embryogenesis.

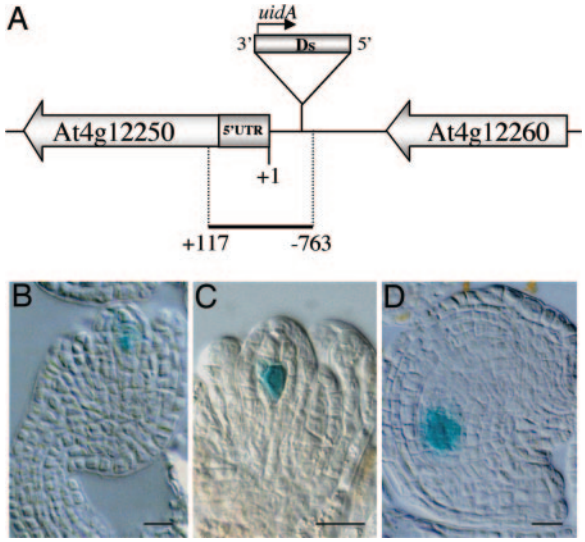

Fig. 5. The pFM1 promoter specifically drives expression during megagametogenesis. (*A*) Genomic localization of the enhancer detector element in ET499. The element inserted in the intergenic region separating At4g112250 and At4g12260 is shown. The numbers indicate the genomic region that was subcloned and used to generate the *pFM1*::*uidA* construct. (*B–D*) GUS expression in developing megagametophytes of *pFM1*::*uidA* transformants. (*B*) GUS expression at the end of megasporogenesis. (*C*) GUS expression in the functional megaspore. (*D*) GUS expression at the micropylar end of a four-nucleate megagametophyte. (Scale bars: 30 μm.)

pFM1 Is a Specific Promoter Driving Expression During Megagametogenesis. ET499 was identified as an enhancer detector line with *uidA* (*GUS*) reporter gene expression in the functional megaspore and the developing megagametophyte (36, 37). A genomic sequence flanking the 3′ border of the enhancer detector *Ds* transposon element was rescued by using thermal asymmetric interlaced

Table 1. Ovule abortion and female gametophyte arrest in *pFM1*::*CHR11*-RNAi lines

pFM1::*CHR11*-RNAi lines	No. of T-DNA insertions	% Aborted ovules	% Female gametophyte arrest*			
			1*N*	2*N*	4*N*	8*N*
T1-17	1	45.0 (67)	45.0 (67)	0	0	0
T1-19	1	44.3 (125)	44.3 (125)	0	0	0
T1-26	ND	51.2 (20)	51.2 (20)	0	0	0
T1-29	1	52.3 (80)	7.3 (11)	13.9 (21)	28.5 (43)	3.3 (5)
T1-32	1	51.4 (127)	36.4 (90)	0.8 (2)	0.8 (2)	0.4 (1)
T1-33	ND	46.8 (81)	45.0 (78)	1.2 (2)	0	0
pFM1-blank	ND	1.1 (2)	0	0	0	0

N, number of haploid nuclei; ND, not determined.
*The number of aborted ovules or arrested gametophytes is shown in parentheses.

PCR. Sequence analysis showed that the *Ds* element was inserted 763 bp upstream of the transcription initiation site of a gene encoding a putative nucleotide sugar epimerase (At4g12250; Fig. 5*A*). We confirmed that the pattern of GUS expression in ET499 reflects the pattern of expression of At4g12250 by showing that a 880-bp genomic fragment (named pFM1) is sufficient to drive reporter gene expression in the functional megaspore in plants transformed with a *pFM1*::*uidA* translational fusion. The genomic region defining pFM1 is composed of the first 763 bp located upstream of the At4g12250 transcription initiation site and the first 117 bp of the transcribed sequence. *pFM1*::*uidA* transformants showed initial GUS expression in the functional megaspore at the onset of megagametogenesis (Fig. 5 *B* and *C*) in the developing megagametophyte (Fig. 5*D*). The pattern of expression persisted in the cellularized megagametophyte but rapidly diminished after double fertilization. GUS expression was absent from all vegetative tissues tested, including seedlings, roots, leaves, stems, and floral organs. These results indicate that pFM1 is a specific promoter acting at the initial stages of megagametogenesis in the functional megaspore and probably drives expression throughout the gametophytic phase of the *Arabidopsis* life cycle.

***CHR11* Is Essential for Haploid Mitotic Progression During Female Gametogenesis.** Although cytological evidence indicates that CaMV35S can often cause RNAi-induced posttranscriptional gene silencing in the developing megagametophyte by acting in the sporophytic cells of the ovule (32), CaMV35S-driven cell autonomous gene silencing has not been demonstrated in the gametophytic phase. Although *CHR11* mRNA is abundantly localized in the megagametophyte, lines in which *CHR11* was posttranscriptionally silenced by using a CaMV35S promoter did not show defects during gametophytic development or early seed formation. To determine the specific function of *CHR11* during megagametogenesis, we replaced the CaMV35S constitutive promoter by pFM1 in the RNAi-inducing plasmid pFGC5941. By transformation through the floral-dip method, 45 primary transformants were generated, none of which showed visible defects during vegetative growth, root development, or floral organogenesis; however, 8 of 45 adult transformants showed semisterility. As shown in Table 1, all *pFM1*::*CHR11*-RNAi lines showed a frequency of ovule abortion between 44.3% (T1-19) and 51.4% (T1-32). Developmental defects in fully penetrant mutants carrying a single insertion and affecting megagametophyte development but not microgametogenesis are expected to occur at a frequency of 50%. Four lines (T2-17, T2-19, T2-29, and T2-32) were selected for subsequent genetic and cytological analysis after determining that these lines contained a single T-DNA insertion, according to Southern blot analysis. Reciprocal crosses to wild-type plants showed that male transmission was normal but that the transmission efficiency of the T-DNA through female gametes was <2% in all four lines tested (data not shown). Semisterile lines had a variable proportion of ovules showing abnormal phenotypes but no obvious defects in pollen formation. All lines underwent normal and synchronized megasporogenesis (Fig. 6 *A* and *F*). After differentiation of the functional megaspore, about half of the ovules divided mitotically three times and gave rise to normally cellularized megagametophytes (Fig. 6 *B–D*), as is observed during wild-type development. By contrast, within the same gynoecium, the nucellus of close to 50% of mature ovules in lines pFM1 T1-17, pFM1 T1-19, and pFM1 T1-26 had a single conspicuous cell closely resembling the functional megaspore (Table 1). Interestingly, this cell enlarged and partially reabsorbed the adjacent nucellar cells (Fig. 6*G*). The three other semisterile lines (including T1-29 and T1-32) showed close to 50% abnormal megagametophytes in which the functional megaspore divided

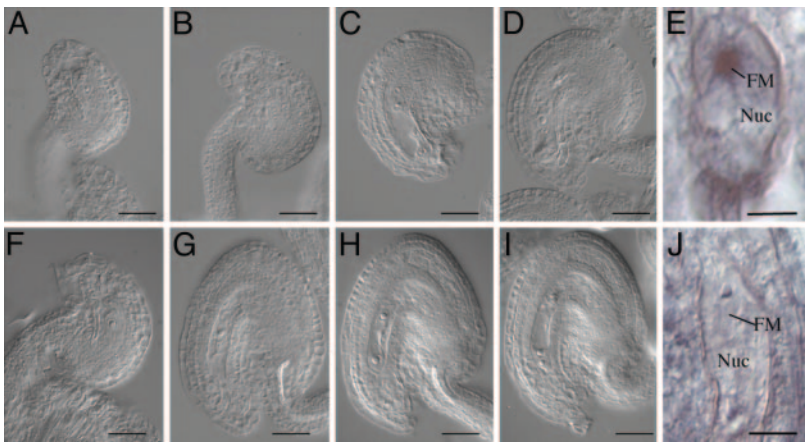

Fig. 6. Megagametophyte development and absence of *CHR11* expression in *pFM1*::*CHR11*-RNAi lines. Wild-type and *pFM1*::*CHR11*-RNAi gynoecia were either fixed, cleared, and viewed under Nomarski optics, or processed for *CHR11* mRNA *in situ* hybridization. (*A–E*) Wild-type ovules; (*F–J*) *pFM*::*CHR11*-RNAi ovules. (*A*) Wild-type ovule at the onset of megagametogenesis. (*B*) Wild-type two-nucleate megagametophyte. (*C*) Wild-type four-nucleate megagametophyte. (*D*) Wild-type cellularized megagametophyte. (*E*) *CHR11* mRNA localization in the functional megaspore of a wild-type ovule. (*F*) Ovule of line T1-29 *pFM1*::*CHR11*-RNAi at the onset of megagametogenesis. (*G*) Mature ovule of line T1-29 *pFM1*::*CHR11*-RNAi showing an arrested one-nucleate megagametophyte. (*H*) Mature ovule of line T1-29 *pFM1*::*CHR11*-RNAi showing an arrested two-nucleate megagametophyte. (*I*) Mature ovule of line T1-29 *pFM1*::*CHR11*-RNAi showing an arrested four-nucleate megagametophyte. (*J*) Absence of *CHR11* mRNA localization in the functional megaspore of a *pFM1*::*CHR11*-RNAi T1-29 ovule. FM, functional megaspore;. Nuc, nucellus. (Scale bars: *A–D*, 30 μm; *E–J*, 10 μm.)

PLANT BIOLOGY

mitotically one (Fig. 6*H*), two (Fig. 6*I*), or three times with no subsequent cellularization. Wild-type plants lacking the *CHR11*-RNAi construct showed normal *CHR11* mRNA localization in the ovule and the developing megagametophyte (Fig. 6*E*). In contrast, the ovule of line pFM1 T1-29 showed *CHR11* expression in sporophytic cells, including the nucellus, but not in the functional megaspore or the developing megagametophyte (Fig. 6*J*), indicating that *CHR11* was specifically silenced in the female gametophytic phase. The frequency of ovule abortion in *pFM1*::*CHR11*-RNAi lines indicates that the phenotype of *pFM1*::*CHR11*-RNAi lines is highly penetrant and gametophytic, with little or no influence from *CHR11* activity that could be provided by diploid sporophytic cells neighboring the developing female gametophyte. Because haploid nuclear proliferation occurs in a syncytium and cellularization takes place after the formation of an 8-nucleate megagametophyte, it is reasonable to suggest that the activity of *CHR11* is cell autonomous during female gametogenesis. Evidence showing that RNAi factors transported from the nucellus are sufficient to cause CaMV35S-driven posttranscriptional silencing in the megagametophyte suggest either that the level of expression of *CHR11* in the sporophytic cells is not sufficient to trigger gametophytic silencing or that factors causing *CHR11* silencing are degraded before reaching the megagametophyte (32).

The activity of ISWI-related remodeling factors has proven essential for modifying the structure of chromatin during reproductive development in several eukaryotic organisms, including yeast (38) and the sea urchin (39). In the mouse, Snf2h$^{-/-}$ embryos show growth arrest at the preimplantation stage, indicating that the activity of this ISWI-related protein is essential for cell proliferation during embryogenesis (40). Our results indicate that *CHR11* regulates similar growth-related programs at several developmental stages of *Arabidopsis* life cycle. A biochemical link between cell expansion and cell cycle regulation has been suggested to depend on the interaction of plant retinoblastoma homologues with members of the E2F family of transcription factors (41). Although several E2F-like genes control the cell cycle in *Arabidopsis* (42), other members, such as AtE2Ff, have been shown to repress cell expansion (43). The retinoblastoma protein and some of its homologues act as suppressors of E2F-like protein activity by recruiting chromatin-remodeling factors of the SWI2/SNF2 family in both plants and animals (41). Remarkably, the retinoblastoma homologue has been shown to control nuclear proliferation in the megagametophyte (44), although several other genes have been also shown to control the gametophytic cell cycle (45–48). An interesting possibility is that *CHR11* could act as a negative regulator of one or several members of the E2F family in the *Arabidopsis*, promoting nuclear proliferation during megagametogenesis and cell expansion during embryogenesis. Although this control could be exerted through the effect of endoreduplication or other mechanisms affecting cell size (49), a detailed elucidation of the cellular pathways regulated by CHR11 will require the determination of its genetic and biochemical interactions with specific molecular partners. Our findings open the possibility of elucidating the specific role that the modification of chromatin structure plays in the development and evolution of the gametophytic phase in flowering plants.

We thank Daphné Autran and Luis Herrera-Estrella for helpful discussions during preparation of the manuscript. This work was supported by Consejo Nacional de Ciencia y Tecnología (CONACYT) Grant B34324 and Z029 and a grant from the Howard Hughes Medical Institute (to J.-P.V.-C.) and, in part, by grants from the Cold Spring Harbor President's Council and the Janggen-Poehn Foundation (to U.G.). W.H.-M. was the recipient of a graduate scholarship from the Organization of American States (OEA) and the Ministry of Foreign Affairs of Mexico. G.L.-M. is the recipient of a graduate scholarship from CONACYT. J.-P.V.-C. is an International Scholar of the Howard Hughes Medical Institute.

1. Emerson, B. (2002) *Cell* **109,** 267–270.
2. Kingston, R. E. & Narlikar, G. J. (1999) *Genes Dev.* **13,** 2339–2352.
3. Becker, P. B., Tsukiyama, T. & Wu, C. (1994) *Methods Cell Biol.* **44,** 207–223.
4. Tsukiyama, T., Becker, P. B. & Wu, C. (1994) *Nature* **367,** 525–532.
5. Aasland, R., Stewart, A. & Gibson, T. (1996) *Trends Biochem. Sci.* **21,** 87–88.
6. Guenther, M. G., Barak, O. & Lazar, M. A. (2001) *Mol. Cell Biol.* **21,** 6091–6101.
7. You, A., Tong, J.K., Grozinger, C.M. & Schreiber, S.L. (2001) *Proc. Natl. Acad. Sci. USA* **98,** 1454–1458.
8. Sterner, D. E., Wang, X., Bloom, M. H., Simon, G. M. & Berger, S. L. (2002) *J. Biol. Chem.* **277,** 8178–8186.
9. Dirscherl, S. S. & Krebs, J. E. (2004) *Biochem. Cell Biol.* **82,** 482–489.
10. Verbsky, M. L. & Richards, E. J. (2001) *Curr. Opin. Plant Biol.* **4,** 494–500.
11. Hsieh, T. F. & Fischer, R. L. (2005) *Annu. Rev. Plant Biol.* **56,** 327–351.
12. Vongs, A., Kakutani, T., Martienssen, R. A. & Richards, E. J. (1993) *Science* **260,** 1926–1928.
13. Kakutani, T., Jeddeloh, J. A., Flowers, S. K, Munakata, K. & Richards, E. J. (1996) *Proc. Natl. Acad. Sci. USA* **93,** 12406–12411.
14. Jeddeloh, J. A., Stokes, T. L. & Richard, E. J. (1999) *Nat. Genet.* **22,** 94–97.
15. Brzeski, J. & Jerzmanowski, A. (2003) *J. Biol. Chem.* **278,** 823–828.
16. Kanno, T., Mette, M. F., Kreil, D. P, Aufsatz, W., Matzke, M. & Matzke, A. J. (2004) *Curr. Biol.* **14,** 801–805.
17. Amedeo, P., Habu, Y., Afsar, K., Scheid, O. M. & Paszkowski, J. (2000) *Nature* **405,** 203–206.
18. Ogas, J., Kaufmann, S., Henderson, J. & Somerville, C. (1999) *Proc. Natl. Acad. Sci. USA* **96,** 13839–13844.
19. Eshed, Y., Baum, S. & Bowman, J. (1999) *Cell* **99,** 199–209.
20. Wagner, D. & Meyerowitz E. M. (2002) *Curr. Biol.* **12,** 85–94.
21. Kwon, C. S., Chen, C. & Wagner, D. (2005) *Genes Dev.* **19,** 992–1003.
22. Farrona, S., Hurtado, L., Bowman, J. L. & Reyes, J. C. (2004) *Development (Cambridge, U.K.).* **131,** 4965–4975.
23. Noh, Y. S. & Amasino, R. M. (2003) *Plant Cell* **15,** 1671–1682.
24. Sambrook, J., Fritsch, E. F. & Maniatis, T. (1989) *Molecular Cloning: A Laboratory Manual* (Cold Spring Harbor Lab. Press, Woodbury, NY), 2nd Ed., pp. 7.43–7.52.
25. Hamillton, A. J. & Baulcombe, D. C. (1999) *Science.* **286,** 950–952.
26. Mette, M. F., Aufsatz, W., Van der Winden, J., Matzke, M. A. & Matzke, A. J. (2000) *EMBO J.* **19,** 5194–5201.
27. Kerschen, A., Napoli, C. A., Jorgensen, R. A. & Muller, A. E. (2004) *FEBS Lett.* **566,** 223–228.
28. Liu, Y. G., Mitsukawa, N., Oosumi, T. & Whittier, R. F. (1995) *Plant J.* **8,** 457–463.
29. Grossniklaus, U., Vielle-Calzada, J.-P., Hoeppner, M. A. & Gagliano, W. B. (1998) *Science* **280,** 446–450.
30. Jefferson, R. A., Kavanagh, T. A. & Bevan, M. W. (1987) *EMBO J.* **6,** 3901–3907.
31. Vielle-Calzada, J.-P., Thomas, J., Spillane, C., Coluccio, A., Hoeppner, M. & Grossniklaus, U. (1999) *Genes Dev.* **13,** 2971–2982.
32. Acosta-Garcia, G. & Vielle-Calzada, J.-P. (2004) *Plant Cell* **16,** 2614–2628.
33. Vielle-Calzada, J.-P., Baskar, R. & Grossniklaus, U. (2000) *Nature* **404,** 91–94.
34. Abramoff, M. D., Magelhaes, P. J. & Ram, S. J. (2004) *Biophotonics Int.* **11,** 36–42.
35. Zimmemrmann, P., Hirsch-Hoffmann, M., Hennig, L. & Gruissem, W. (2004) *Plant Physiol.* **136,** 2621–2632.
36. Sundaresan, V., Springer, P., Volpe, T., Haward, S., Jones, J. D., Dean, C., Ma, H. & Martienssen, R. (1995) *Genes Dev.* **9,** 1797–1810.
37. Grossniklaus, U., Moore, J. M., Brukhin, V., Gheyselinck, J., Baskar, R., Vielle-Calzada, J.-P., Baroux, C., Page, D. R. & Spillane, C. (2003) *Plant Biotechnology 2002 and Beyond*, ed. Vasil, I. (Kluwer, Dordrecht, The Netherlands), pp. 309–314.
38. Gelbart, M. E., Bachman, N., Delrow, J., Boeke, J. D. & Tsukiyama, T. (2005) *Genes Dev.* **19,** 942–954.
39. Medina, R., Gutierrez, J., Puchi, M., Imschenetzky, M. & Montecino, M. (2001) *J. Cell Biochem.* **83,** 554–562.
40. Stopka, T. & Skoultchi, A. (2003) *Proc. Natl. Acad. Sci. USA* **100,** 14097–14102.
41. Reyes, J., Hennig, L. & Gruissem, W. (2002) *Plant Physiol.* **130,** 1090–1101.
42. De Velyder, L., Beeckman, T., Beemster, G. T. S., de Almeida Engler, J., Ormenese, S., Maes, S., Naudts, M., Van Der Schueren, E., Jacqmard, A., Engler, G. & Inzé, D. (2002) *EMBO J.* **21,** 1360–1368.
43. del Pozo, J. C., Boniotti, M. B. & Gutierrez, C. (2002) *Plant Cell* **14,** 3057–3071.
44. Ebel., C., Mariconti, L. & Gruissem, W. (2004) *Nature* **429,** 776–780.
45. Springer, P. S., McCombie, W. R., Sundaresan, V. & Martienssen, R. A. (1995) *Science* **12,** 877–880.
46. Pischke, M. S., Jones, L. G., Otsuga, D., Fernandez, D. E., Drews, G. N. & Sussman, M. R. (2002) *Proc. Natl. Acad. Sci. USA* **99,** 15800–15805.
47. Kwee, H. S. & Sundaresan, V. (2003) *Plant J.* **36,** 853–866.
48. Shi, D.-Q., Liu, J., Xiang, Y.-H., Ye, D., Sundaresan, V. & Yang, W.-C. (2005) *Plant Cell* **17,** 2340–2354.
49. Sugimoto-Shirasu, K. & Roberts, K. (2003) *Curr. Opin. Plant Biol.* **6,** 544–553.